

A. KUMAR<sup>1\*</sup>, D. DAS<sup>1</sup>, N.D. RAJ<sup>1</sup>, S. BAG<sup>1</sup>, V.C. SRIVASTAVA<sup>2</sup>

## COMPARISON OF MACHINE LEARNING PERFORMANCE FOR THE PREDICTION OF MELTING EFFICIENCY AND BEAD GEOMETRY IN WIRE ARC ADDITIVE MANUFACTURING PROCESS

Wire arc additive manufacturing (WAAM) is amongst the emerging technologies of the layer-by-layer deposition process to manufacture the metallic parts. Multi-layer bead deposition using the WAAM process leads to the fabrication of complex products with practical utility. The bead profile of each layer controls the geometry of the final product. However, the melting efficiency and the bead geometry depend on the various process parameters. The primary process parameters affecting the melting efficiency and the bead geometry are the wire feed rate, travel speed, diameter of the wire, and power. Owing to the various complexities during metal deposition, predicting the dimensions at each deposition attribute is not always feasible. Hence, the current work is focused on the utilization of different machine learning (ML) algorithms to understand the relationship between the process parameters, melting efficiency, and bead geometry. The different ML models used for the current work are linear regression (LR), decision tree regressor (DTR), random forest (RF), support vector regression (SVR) and, extra tree regressor (ETR). The ETR is found to predict the melting efficiency with the highest prediction rate of 97.4%, whereas, the SVR and LR predict the bead width and height with the highest accuracy rate of 97.4% and 98.7%, respectively.

*Keywords:* WAAM; bead geometry; melting efficiency; machine learning regression models; hyperparameter tuning

### 1. Introduction

Additive Manufacturing (AM) is an advanced manufacturing technique utilized for fabricating components in a layer-by-layer fashion using a STL file developed from a CAD model. Its popularity is by virtue of its advantage over conventional manufacturing processes in terms of design freedom and ability to manufacture complex geometries. AM has been commercially adopted for use in high-tech industries such as healthcare for custom implants, aerospace for lightweight designs, automotive, civil construction, and energy production [1-4]. Although AM has attracted a lot of interest in the industrial and academic sectors, accelerating the production rate, volume, and quality of printed goods production remains a significant problem [5]. Commonly, metallic parts can be produced by AM technologies by using the techniques like wire arc additive manufacturing (WAAM), Electron beam freeform fabrication (EBF), Selective laser melting (SLM), Selective laser sintering (SLS), and Electron beam melting (EBM). Welding wire is used as a feedstock material and an electric arc serves as the heat source for melting in WAAM process. It can manufacture massive components with great efficiency and

little expense [6]. It can fabricate near-net-shape products without complex tooling, moulds, or dies. Gas metal arc welding, gas tungsten arc welding, and plasma arc welding are the three predominant processes that are extended to WAAM technologies [7].

The required product is directly printed layer-by-layer through the elimination of several conventional manufacturing processes. Each layer has a bead profile that ultimately determines the physical features of the printed product. A major concern in the existing WAAM technology is that the quality of the final printed product is not consistent, which is highly dependent on various processing parameters, such as deposition speed, current, voltage, travel speed, wire feed, and stick-out length [8,9]. The width of the bead and the penetration depth decreases with an increase in the travel speed [10]. The wire feed does not significantly affect the depth of penetration and surface roughness. However, the ratio of the wire feed to the travel speed can substantially influence the width, height, and depth of penetration [11]. In effect, the travel speed, current, and current polarity remarkably influence the shape of a 3D-printed bead. Straight polarity and higher current provide larger reinforcement areas which in turn reduce the cooling rate of the metal and reduce

<sup>1</sup> INDIAN INSTITUTE OF TECHNOLOGY GUWAHATI, DEPARTMENT OF MECHANICAL ENGINEERING, INDIA

<sup>2</sup> MATERIALS ENGINEERING DIVISION, CSIR-NATIONAL METALLURGICAL LABORATORY, JAMSHEDPUR, INDIA

\* Corresponding author: [amritesh.kumar@iitg.ac.in](mailto:amritesh.kumar@iitg.ac.in)



the weld dilution [12]. Depth of penetration usually increases with an increase in welding current, reaches an optimum point, and reduces further with an increase in current [13]. However, welding current, cooling time, and interlay temperature affect the surface finish and dimensional accuracy [14]. Literature indicates that natural cooling time and idle time do not significantly affect the properties of the deposited WAAM layer [15, 16].

The causative variables such as temperature gradient and cooling rate are controlled by the heat input. Hence, the heat input is an important parameter of the WAAM process. Fuer-schbach et al. [17] have pointed out that the heat input alone cannot determine the amount of metal melted during deposition. The energy that goes into the material and out of the deposition centreline, due to heat dissipation, is a significant loss for melting of the material [18]. Therefore, the melting efficiency is used to characterize this heat loss and is defined as the ratio of the minimum heat required for the fusion and the actual energy consumed. Melting efficiency also depends on the width of the heat affected zone [19]. The melting efficiency can be measured accurately using calorimetric techniques, but they do not account for losses that occur between the start of the operation and the measurement [20]. Various numerical models have been developed based on the physics of the process [21]. However, the solution of the Navier-Stokes equation increases the computation cost involved. AM research has experienced a paradigm change in favour of a mix of physics-based and data-driven techniques due to the complicated multi-physics and multi-scale nature of AM processes and the impact of different process factors on the quality of the produced product [22].

The conventional forecasting techniques are incapable of predicting, and establishing the physical responses with varying process parameters of the AM processes [13]. Therefore, in the recent past, various Artificial Intelligence approaches such as machine learning (ML), Artificial Neural Networks (ANN), and deep learning based on data-driven analysis are applied to AM processes [23,24]. Abdullah Al-Faruk et al. [13] developed an ANN-based model that can be used successfully to predict output parameters like bead height, bead width, and depth of penetration. But the errors can be high in some cases, like predicting bead width. Increasing the number of hidden layers, data sample size, and iterations can minimize this error [13]. Pradhan et al. developed Linear Regression (LR) and ANN models to predict the dimensions of weld beads like throat height, leg length, width, and penetration. LR model developed produced much better results as compared to the ANN model. Barrionuevo et al. [26] developed various ML models like Gaussian process regression (GPR), Extreme gradient boosting regressor (XGBR), and Multi-layer perceptron (MLP) to accurately predict the melting efficiency with various process parameters. It was reported that the accuracy in all these cases was around 85%.

Based on the extensive literature survey, it has been observed that various works related to bead geometry for AM and especially WAAM have been reported, but studies which can correlate the physical dimensions of the bead deposited and the melting efficiency of the process with the input process param-

eters and accurately predict them are scarce. This gap has been addressed in the current article with the help of ML algorithms. This work aims to develop different ML models to predict the outcome of WAAM deposition. As, we know that the prediction accuracies of the ML models depend on the levels of the complexity of problem depicted by the datasets, and acquiring the domain knowledge of the problems while training. Based on the datasets, several ML models are developed. Hence, before deploying the best models for the prediction, multiple ML algorithms must be fitted and compared to obtain the best accuracy and low errors for the prediction. For our analysis, SVR (for the prediction of width) and, ETR (for the predictions of melting efficiency) provides the best result. The accurate prediction of the bead geometry and melting efficiency will further improve the acceptance of WAAM in the manufacturing industry.

## 2. Machine learning models

### 2.1. Importing dataset and cleaning the data

Data is the most important asset of any ML model. Volume and quality of data directly affect the accuracy and efficiency of the ML regression model developed. Cleaning the data includes validating the datatype (integer, characters, float, etc.) and filtering the data entries with structural errors. This is important as the data is acquired from different sources and it might contain inconsistent data points. This can give rise to undue errors in the output results.

### 2.2. Check for outliers and build basic intuition

Outliers can exist in any data which may be caused by multiple reasons. But it is crucial to weed out any such outliers at the early stage i.e., before using them for ML. If the model starts considering the data which are not correct and out of range, the predictions will lose their accuracy. Hence, it is important to identify the data that are outliers and treat them suitably before reconsidering them. Generally, the outlier data points are taken off the dataset. A boxplot depicts the data in the form of five numeric summaries helping in the visualization of dispersion and skewness of the available data points [27]. Basic intuitions are then formed around the data given. Visualization helps to understand the data better and acts as an aid to make further decisions. Various plots like pair plots, and correlation matrix (heat map) are plotted to understand the data better before building an appropriate ML regression model.

### 2.3. Splitting the data into the training set and testing set

Any ML model developed needs to be tested before finalizing. For the same purpose, the available dataset is divided into

two categories. The training dataset is used for developing and training the model. The larger chunk of data is split into this category, usually, about 75-90% as this determines the quality of the ML model developed. The other set of data is not made available for the model as it is strictly used only to test and validate the accuracy of the ML model. This is done before proceeding to further steps to avoid any data leakage and preserve the test data for validating the developed regression model.

## 2.4. Feature scaling

Given that a dataset might contain numbers of different orders, it becomes difficult for an ML model to deal with them. If the distance between data points is large, it can lead to erroneous results. To reduce the errors and help the ML model predict better, feature scaling is done. Feature scaling ensures that all the data points available are in a certain range. Feature scaling is done after splitting the data to avoid any data leakage. Splitting before feature scaling ensures that the training dataset is completely independent of the testing dataset and there is no bias induced. The range is decided by the feature scaling model that is chosen. Largely, there are two types of feature scaling.

### 2.4.1. Normalization:

It keeps the data between  $[0,1]$  using a minmax scalar. The relationship used for normalization is given below.

$$X_{norm} = \frac{X - X_{min}}{X_{max} - X_{min}} \quad (1)$$

where  $X_{norm}$  is the normalized feature value,  $X$  is the feature value,  $X_{min}$  is the minimum feature value, and  $X_{max}$  is the maximum feature value.

### 2.4.2. Standardization:

The process of rescaling the features to give them the characteristics of a Gaussian distribution with  $\mu = 0$  and  $\sigma = 1$ , where  $\mu$  is the mean and  $\sigma$  is the standard deviation from the mean, is known as standardization (or Z-score normalization). The following formula is used to determine the samples standard scores, often known as z-scores:

$$z = \frac{x - \mu}{\sigma} \quad (2)$$

## 2.5. Development of the ML models

As there is no thumb rule established regarding the model to be chosen for a particular kind of dataset, it is necessary to implement various regression models to check the best fit. Hence, importing and trying all the appropriate regressors are the best way to come up with the most accurate ML model. Multiple Linear Regression (MLR), Support Vector Regression (SVR), Lasso Regressor (LR), Random Forest Regressor (RFR), Extra

Tree Regressor (ETR) etc. are a few regressors available for developing an ML model. MLR is the most commonly used algorithm and it's fundamental for several other models. Mathematically it can be expressed as follows:

$$y(x) = a_0 + a_1x_1 + a_2x_2 + \dots + a_nx_n \quad (3)$$

where  $y$  is the output variable,  $x_1, x_2, \dots, x_n$  are the input features, and  $a_0, a_1, \dots, a_n$  are the parameters that need to be evaluated while model training using suitable optimization algorithm like gradient descent. Solution of the problem by SVR consists of transferring the training datasets into high order dimensions that leads to the establishment of hyperplane and its separation. Let us assume that  $X = [X_1, X_2, \dots, X_n]^T$  be the input features, and  $Y = [Y_1, Y_2, \dots, Y_n]^T$  are the output variable. Regression equation pertaining to these variables is given by:

$$y(x) = w \cdot \phi(x) + b \quad (4)$$

where  $y(x)$  depicts the output function,  $w$  is the weight coefficient,  $b$  is bias, and  $\phi(x)$  is the non-linear function that converts the datasets into high order dimension. According to the training set, DTR model generates a decision tree that predicts the specific output which in turn depends on the input features. Depending on the types of problem (classification or regression), CART (classification and regression tree) algorithm changes. Based on these algorithm, binary trees are constructed. Working principle of this algorithm is such as: at particular node, subset of training data ( $N_{node}$ ) is divided into two parts –  $N_{node}^{left}(S)$  and  $N_{node}^{right}(S)$ ; hence it is called as split  $S$ . Further dependency of  $S$  is on certain factor ( $f$ ) with particular threshold  $t_{node}$ ; and  $x_f$  be the feature at node. Hence, mathematical formulation is given by:

$$S = (f, t_{node}) \quad (5)$$

$$N_{node}^{left}(S) = \{(x, y) | x_f \leq t_{node}\} \quad (6)$$

$$N_{node}^{right}(S) = N_{node} \setminus N_{node}^{left}(S) \quad (7)$$

Further, the impurity at split is evaluated according to Eq. (x) that leads to the utilization of loss function for regression problems. The main purpose of CART algorithm is to minimize the impurity at each node. Mathematical equations for the predicted output of regression problem is given by:

$$\bar{y}_n = \frac{1}{N_n} \sum y \in N_i y \quad (8)$$

$$W(Q_n) = \frac{1}{N_n} \sum y \in N_i (y - \bar{y}_i)^2 \quad (9)$$

$$I(N_{node}, S) = \frac{N_{node}^{left}}{N_{node}} \cdot W(N_{node}^{left}(S)) + \frac{N_{node}^{right}}{N_{node}} \cdot W(N_{node}^{right}(S)) \quad (10)$$

Where  $Q_n$  is utilized subset of training data,  $N_n$  is the number of training sample in  $Q_n$ ,  $y$  depicts the output, and  $\bar{y}_n$  is the mean

value of all the output. This complete process is repeated till maximum depth of tree is obtained or ly one sample at node is left out.

RFR model is an ensemble learning techniques that consists of generating forest of multiple decision trees and finally computes the mean value of each tree and gives the predicted value. ETR model is also an ensemble learning techniques that gives the prediction based on the number of decision trees. Hence, the mathematical formulation of this model based on the DTR. Initially the ETR model was developed from RF algorithm. This algorithm gives higher prediction accuracy for the smaller size of datasets as it utilized the complete training set for the optimization of the branches of decision tree.

### 2.5.1. Hyperparameter tuning

Every ML model has certain parameters for performing the required operations. They are unique to each regressor and decide the accuracy and efficiency of the model developed. These parameters are called hyperparameters. They define the model and its working. The hyperparameters can be tuned to obtain better performance from the model. A few of the hyperparameters for different regressor models are given in TABLE 1.

TABLE 1

Few of the regression models and their hyperparameters

Regressor	Hyperparameters
Ridge regressor	Maximum iterations, tolerance, solver
Support vector	Kernel type, Degree of the polynomial kernel function, Kernel coefficient, tolerance
Decision Tree regressor	Criterion, the maximum depth of the tree, splitter used

### 2.5.2. Check the performance and verify the results

The accuracy of the model developed is measured by two parameters viz.  $R$ -squared score (or score) and mean squared error (MSE).  $R$ -squared ( $R^2$ ) is widely used to measure the goodness of fit. Nonlinear models generally lead to a value that can lie beyond  $[0,1]$  interval and reduce as regressors are added [28]. Mathematically,  $R^2$  score is,

$$R^2 = 1 - \frac{\text{Unexplained Variation}}{\text{Total Variation}} \quad (11)$$

$$R^2 = 1 - \frac{\sum (y_i - \hat{y}_i)^2}{\sum (y_i - \bar{y})^2} \quad (12)$$

Where,  $y_i$  is the predicted value,  $\hat{y}_i$  is the actual value, and  $\bar{y}$  is the mean value.  $R$ -squared scores of 0.97 and above are considered good and can be deduced that the developed model is able to predict the required data accurately.

The degree of inaccuracy in statistical models is gauged by the mean squared error, or MSE. Between the observed and

projected values, it evaluates the average squared difference. It is mathematically represented by the following formula.

$$MSE = \frac{\sum (y_i - \hat{y}_i)^2}{n} \quad (13)$$

Where,  $y_i$  is the predicted value,  $\hat{y}_i$  is the actual value, and  $n$  is the number of observations. The model can alternatively be verified using a few known data points. The model can be used to predict data that is known and can be validated using the ML model developed.

## 2.6. Dataset of the process

### 2.6.1. Bead dimensions

The bead profile is defined by two major dimensions i.e., bead width and bead height (Fig. 1). These dimensions decide the quality and the accuracy of the product built. But several parameters contribute to the outcome of the bead profile. Hence, it is difficult to predict the exact dimensions that will be obtained. To develop the ML model, we used the dataset from the research paper published by Ding et al. in the year 2015 [29].

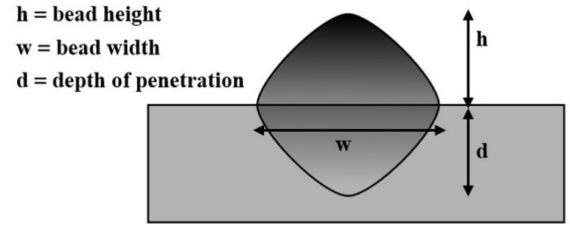


Fig. 1. Schematic of weld bead geometry

In the experiments conducted by them, the varying deposition attributes are wire feed, travel speed, and stick-out length. Minimum and maximum values for wire feed rates are varies from 5 m/min-7 m/min, travel speed varies from 0.35 m/min-0.7 m/min, and stick out length varies from 9 mm-15 mm. Bead width and height are measured and considered as output values. A few of the experimental values obtained from the research paper are shown in the TABLE 2.

### 2.6.2. Melting efficiency

Accurate prediction of the melting efficiency is essential as it signifies the efficiency of the whole process. To manifest the same, an ML model is developed using the dataset available in the research paper published by Barrionuevo et al. [26]. In this study, wire feed rate, travel speed, diameter of the wire, and power employed as a deposition parameter for the fabrication of mild steel products by cold metal transfer. For this dataset, wire diameter varies from 0.8 mm-1.2 mm, wire feed speed ranging from 28 mm/s-222.5 mm/s, travel speed varies from 1.66 mm/s-25 mm/s, and power from 531.2 W-3266.5 W. A set

TABLE 2

Sample of welding process input parameters and the responses obtained [29]

Parameters			Responses	
Wire feed (m/min)	Travel speed (m/min)	Stick out (mm)	Height (mm)	Width (mm)
5	0.35	9	3.43	6.74
5	0.46	11	2.96	5.97
5.7	0.58	15	2.57	6.19
5.7	0.7	13	2.21	5.7
6.4	0.35	13	3.42	8.53
6.4	0.46	15	2.91	7.53
7	0.35	15	3.21	9.22
7	0.7	9	2.29	7.28
6	0.5	12	2.75	7.04
6.5	0.6	10	2.5	7.27
5.5	0.4	11	2.94	7.34
5.8	0.48	11	2.56	7.12
6.2	0.52	10	2.49	7.45
6.2	0.7	11	2.17	6.65

TABLE 3

Dataset sample from Barrionuevo et al. [26]

Wire Diameter (mm)	Wire Feed (mm/s)	Travel speed (mm/s)	Power (KW)	Melting Efficiency
0.8	39.33	5	531.22	0.396
0.8	48.33	6.66	693.84	0.414
0.8	122.5	14.99	1727.29	0.482
0.8	137.17	16.67	1921.5	0.474
0.8	42	3.33	550.86	0.376
0.8	112.67	7.51	1714.14	0.422
1	89	6.67	2064.77	0.467
1	57	3.33	1407.78	0.394
1	71.17	4.17	1788.14	0.412
1	90.5	5	2068.2	0.453
1	100.33	5.83	2323.55	0.466
1.2	47.67	6.68	1737.51	0.41
1.2	55.17	8.33	1970.48	0.428
1.2	44.33	3.34	1688.92	0.372
1.2	57.33	4.17	1996.29	0.446
1.2	89.33	6.67	2887.92	0.5

of 75 experiments were conducted and the results were recorded. A few of the data points are shown in TABLE 3. All the steps involved (data pre-processing, hyperparameter tuning of model parameters, and model fitting) in the development of machine learning models were accomplished by utilizing scikit-learn library available in python programming language.

### 3. Results and discussions

The data was pre-processed and checked for any non-permissible values. The outliers were checked using the boxplot. The boxplot of various input parameters viz. The wire feed, travel speed, and stick-out length based on the experiments of Ding et al. are shown in Fig. 2.

Once data munging was completed, basic intuitions were built using graphs showing variations in output parameters with the input variables and a correlation matrix. Wire feed and stick-out length do not have a noticeable control over the height of the bead as observed in Figs. 3a and 3c, respectively. Also, it is observed from Fig. 3b that travel speed has a significant impact on the height of the deposited bead layer. In Fig. 4, bead width was plotted against various input variables. Wire feed and travel speed contribute significantly towards determining the width of the bead profile deposited as observed in Figs. 4a and 4b, respectively. It was observed that the stick-out length does not have any impact on the width of the bead as it is less correlated (0.046) (Fig. 5).

These intuitions can be further strengthened by studying the correlation matrix plotted in Fig. 5. Observing the fourth row of the correlation matrix, we can note the different correlation

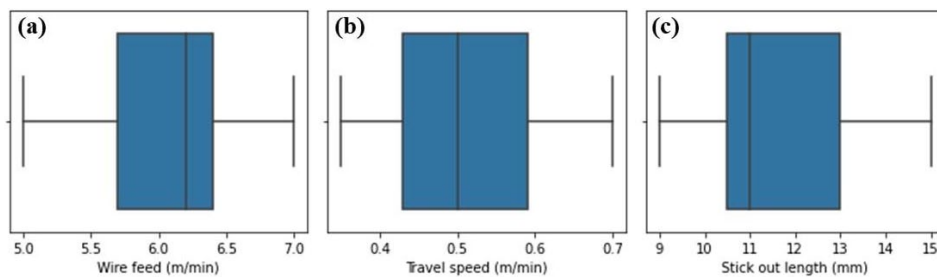


Fig. 2. Boxplot of the process parameters viz. Wire feed (a), Travel speed (b), and Stick out length (c) are involved in predicting the bead dimensions

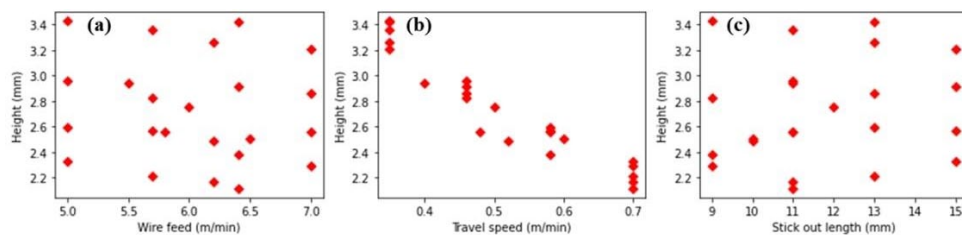


Fig. 3. Variation of the height of bead geometry with (a) wire feed (a), (b) travel speed, and (c) stick-out length

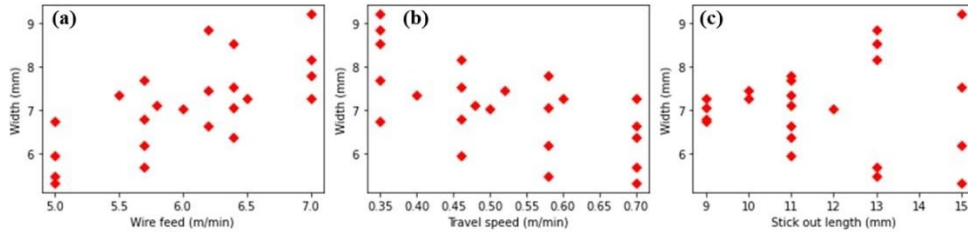


Fig. 4. Variation of the width of bead geometry with (a) wire feed, (b) travel speed, and (c) stick-out length

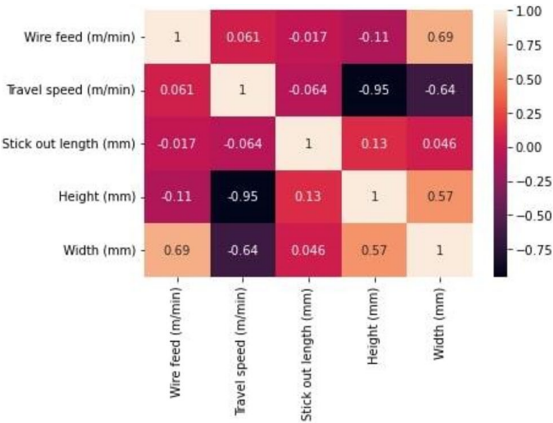


Fig. 5. Correlation matrix denoting the relation between height and width of bead geometry and the input parameters

coefficients pertaining to the height of the bead profile. The correlation coefficient of height corresponding to the travel speed is

-0.95 depicting the idea that the travel speed affects the height of the bead inversely. The magnitude of the correlation coefficients between height and the wire feed, and stick-out length are small, conveying the fact that they have a minimum effect on the output i.e., the height of the deposited layer. Similarly, the fifth row contains the correlation coefficients of width with varying process parameters. The width of the deposited layer has correlation coefficients that signify that the wire feed (0.69) affects the width in a quasi-linear manner whereas it decreases with the increasing travel speed (-0.64).

Similarly, the boxplot is visualized for all the process parameters used in determining the melting efficiency in Fig. 6. The wire diameter (Fig. 6a), wire feed (Fig. 6b), and power (Fig. 6d) have a typical graph generated as opposed to an unusual plot of travel speed. In Fig. 6c it can be seen that three data points lie beyond the third quartile line (Q3). Q3 denotes the median of the second half of the data. This is not a concern as we are aware of the fact that it is well within the limits and is not an

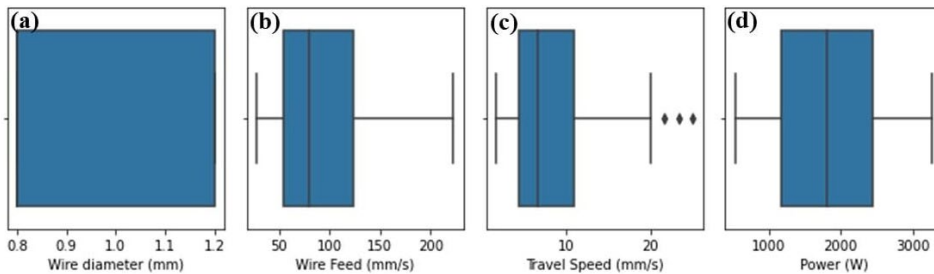


Fig. 6. Boxplot of the process parameters: (a) wire diameter, (b) wire feed, (c) travel speed, and (d) power involved in predicting the melting efficiency

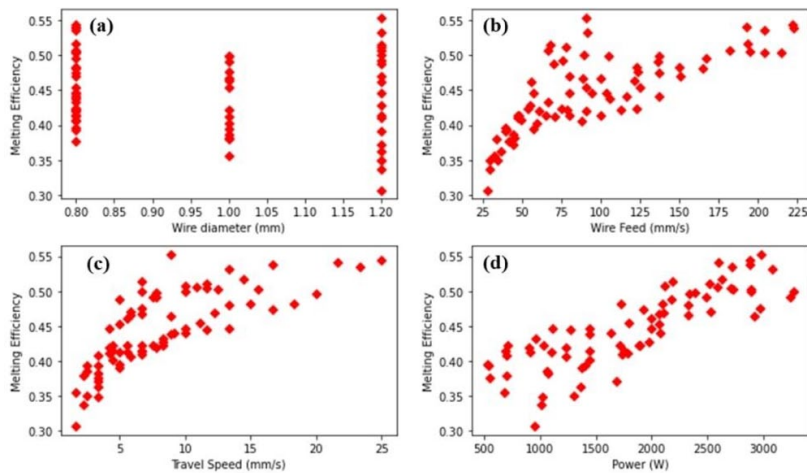


Fig. 7. Variation of melting efficiency with (a) wire diameter, (b) wire feed, (c) travel speed, and (d) power

erroneous entry. It is a slight deviation that will not affect our model in any manner.

Melting efficiency is plotted against the process parameters used viz. wire diameter, wire feed, travel speed, and power. The basic intuition drawn from the plots is that melting efficiency is affected by the process parameters like wire feed, travel speed, and power whereas it is fairly independent of the wire diameter. The melting efficiency is seen to be increasing almost linearly with wire feed, travel speed, and power.

The correlation matrix is developed for the melting efficiency and its process parameters. The last row contains all the correlation coefficients with respect to melting efficiency. It aids in building the idea that wire diameter is not affecting the melting efficiency as its correlation coefficient is as low as  $-0.15$ . Also, the correlation coefficients of wire feed, travel speed, and power are  $0.76$ ,  $0.76$ , and  $0.83$  respectively. It can be concluded that as the coefficients are approaching 1, the relationships are highly dependent i.e., melting efficiency is highly dependent on wire feed, travel speed, and power.

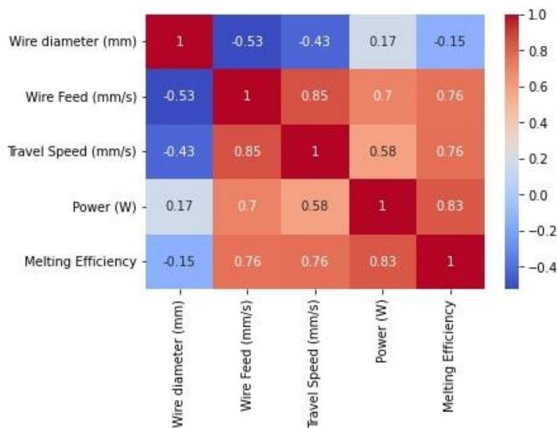


Fig. 8. Correlation matrix denoting the relation between melting efficiency and the input parameters

The data was then randomly split in the ratio of 4:1 into training and testing, respectively. Once the data is split, the training data is subjected to feature scaling. Various regression models were developed and their accuracies were examined. The regression models used were Linear Regression (LR), Support Vector Regression (SVR), Ridge Regression (RR), K-Nearest Neighbours (KNN), Random Forest Regression (RFR), and Extra Tree Regression (ETR). Hyperparameters utilized while fitting models are depicted in TABLE 5. The procedure for tuning the hyperparameter is gridsearchcv. The gridsearchcv considers all the possible permutations and combinations of parameters before optimizing the parameter values within the given range.

### 3.1. Prediction of bead dimensions

The  $R^2$  score and MSE of various models developed for predicting the height of a deposited bead with varying input parameters are shown in Fig. 9 and Fig. 10 respectively.

Scores of different models for prediction of height

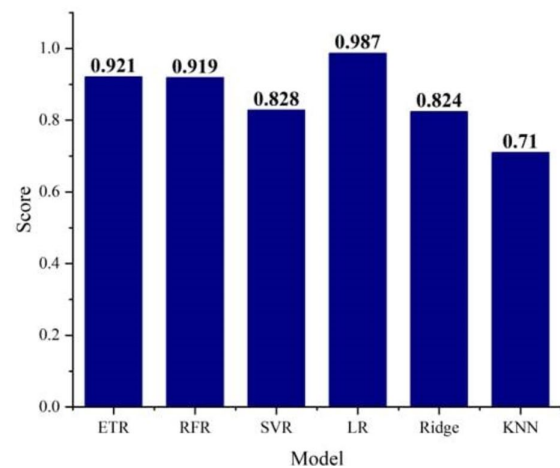


Fig. 9. Scores obtained by different regressors predicting the height of the bead

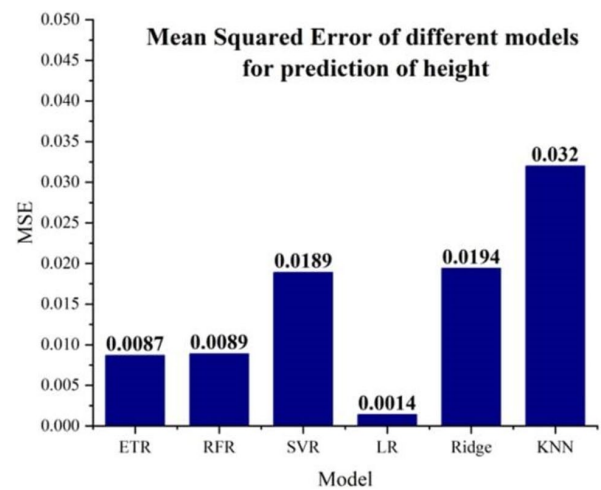


Fig. 10. MSE obtained by different regressors predicting the height of the bead

It is observed that the LR model is performing the best to predict the height of the deposited bead layer. The  $R$ -squared score of the LR model is around 0.987 and its corresponding MSE is as low as 0.0014. The other models like ETR and RFR have scores around 0.92 which are satisfactory. With a score of 0.987, the LR model is finalized to predict the bead height.

Figs. 11 and 12 show the  $R^2$  score and MSE of different regressor models developed for predicting the width of a deposited bead with varying input parameters. SVR and LR are two of the best-performing models for predicting the width of the deposited bead layer. Their scores are 0.974 and 0.963 respectively. Their MSE values are 0.0257 and 0.0365 respectively. It is evident that SVM has an edge over LR in predicting the width of the bead profile. Non-linearity of the datasets was solved using the radial basis function as the kernel tricks by SVR model. Hence, it achieves the highest prediction accuracy on fitting of the bead width dimensions. SVR with an  $R$ -squared score of 0.974 is recommended for the task of predicting the width.

Scores of different models for prediction of width

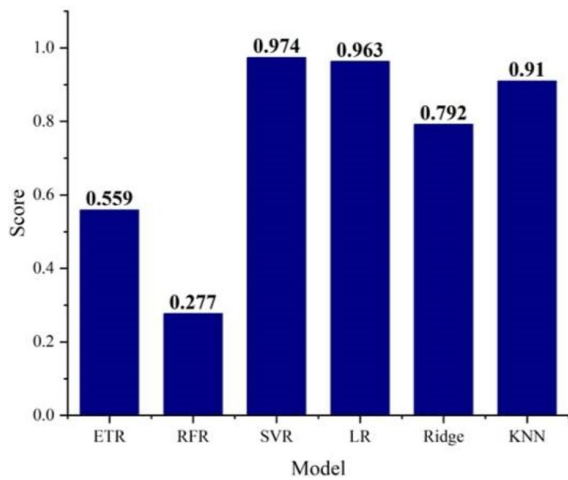


Fig. 11. Scores obtained by different regressors predicting the width of the bead

Mean Squared Error of different models for prediction of width

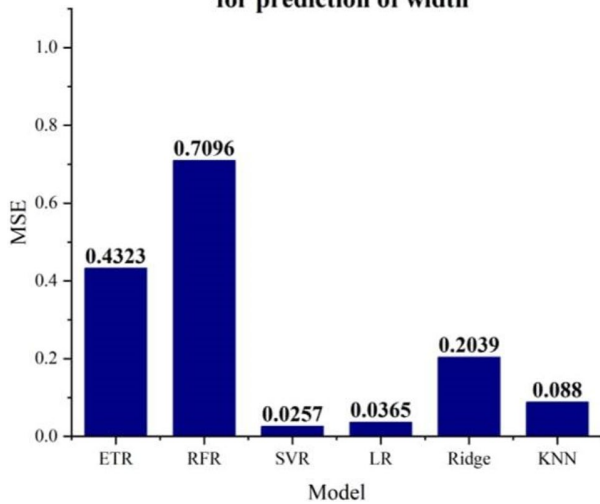


Fig. 12. MSE obtained by different regressors predicting the width of the bead

A few of the results are compared in TABLE 4. It can be seen that the models are working efficiently with very minimal deviation from the actual dimensions of height and width of the deposited bead layer.

TABLE 4

Comparison between the model prediction vs actual dimensions

Sl no.	Actual height (mm)	Predicted height (mm)	Actual width (mm)	Predicted width (mm)
1	2.17	2.16	6.65	6.55
2	2.59	2.58	5.48	5.58
3	2.57	2.58	6.19	6.11
4	2.91	2.93	7.53	7.63
5	2.56	2.50	7.79	7.66
6	2.56	2.64		7.15

### 3.2. Prediction of melting efficiency

Various regression models were employed to arrive at the most accurate ML model that could predict the melting efficiency of the process with varying process parameters. The  $R^2$  scores of various ML regressor models developed can be seen in Fig. 13. Their respective MSE observed is shown in Fig. 14. Initially, it was seen that the ETR model is producing the best results with a score of 0.958. The next nearest best-performing model is RFR with a score of 0.931. The ETR model provides the best prediction for the melting efficiency as it consists of mean value as a predictor value from the multiple decision trees.

Scores of different models for prediction of melting efficiency

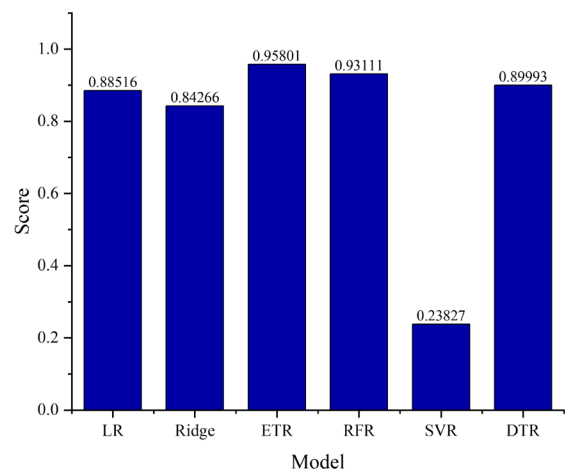


Fig. 13. Scores obtained by different regressors predicting the melting efficiency

Mean Squared Errors of different models predicting the melting efficiency

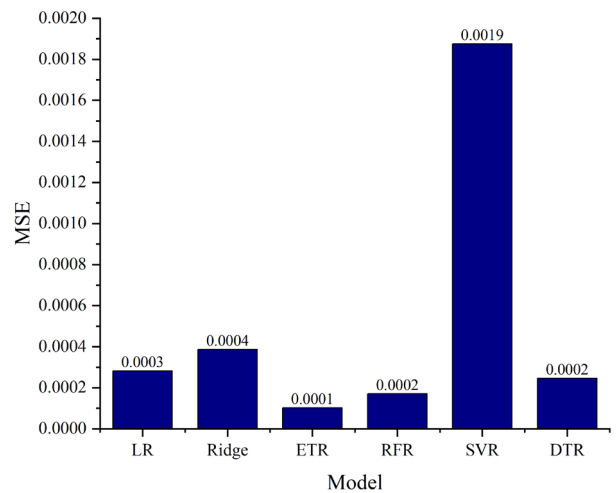


Fig. 14. MSE obtained by different regressors predicting the melting efficiency

After identifying the top three regressors, each regressor is subjected to hyperparameter tuning to have the best-fitting model. The parameters like the number of estimators, criterion, splitter, etc. were tuned as per the given data set and a model was

developed which can most accurately make the predictions. After multiple iterations, it was deduced that the Extra Tree Regressor with the following hyperparameters produced the best results. TABLE 5 shows the best hyperparameters of ETR for predicting the melting efficiency.

TABLE 5

Best hyperparameters obtained for extra tree regressor (ETR)

Models	Hyperparameters utilized for model	Parameters
ETR	No. of estimators	5
	Random state	5
	Criterion	MSE
	Minimum sample split	2
	Minimum samples leaf	1
RFR	Criterion	MSE
	Maximum depth	7
	Number of estimators	50
	Random state	11
SVR	Kernel	Rbf
	C	100
KNN	No of neighbours	5
	Leaf size	30

A score of 0.974 was obtained with the above-mentioned hyperparameters which predict the melting efficiency of the process with an MSE of  $6.52 \times 10^{-5}$ . This ETR model is superimposed for accurate prediction of melting efficiency. From Fig. 15, it can be convincingly concluded that the developed ETR model fits the data obtained from research paper very accurately.

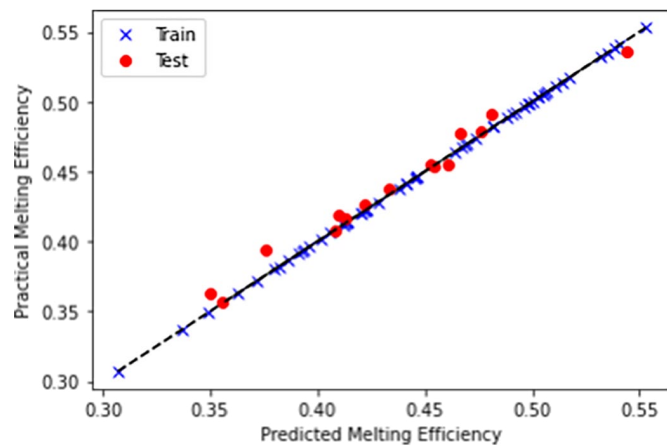


Fig. 15. Comparison between predicted and actual melting efficiency

#### 4. Conclusions

For the fabrication of components by WAAM process, deposition attributes like travel speed, heat input, wire feed speed, and wire diameter play a paramount role in deciding the product dimensions and its functionality. These variants must be selected properly using proper design of experiments. However, conducting experiments at various levels of attributes and deciding the optimal values by trial and error are time consuming and increases the overall production cost. Hence, in this study various

ML models are trained on the experimental data available from the independent literature. Further, the best models are utilized for the prediction. A total of three ML Regression models are developed for accurately and efficiently predicting the height and width of the deposited bead profile, and the melting efficiency of the process. There are several input process parameters that vary to give diverse output values. Regressors like LR, SVR, RFR, Ridge, and DTR are used to arrive at the best possible model to achieve the target of predicting the physical dimensions of the bead and the melting efficiency of the process. LR is used to predict the height of the bead profile with a score of 0.987. SVR is employed to predict the width of the bead deposited having a score of 0.974. However, ETR produces the best results for predicting the melting efficiency of the process among all the regressors with a score of 0.958. Upon tuning the hyperparameters, the final ETR model had a score of 0.974. The drawback with this model is that it is based on very limited data points and thus produces deviations from the actual values. This can be rectified by increasing the volume of data available for the model to learn, understand, and strengthen the understanding of the relationships between the output parameters and the input process parameters. It is not required to design all the deposition attributes, rather than, its influence on the output can be evaluated by feature importance and further it is predicted based on their significance level on the output. The current work can be further extended to develop more efficient ML models on our experimental datasets as a digital twin that can predict both deposition parameters (inverse predictions of variants from the targeted melting efficiency and bead dimensions), and bead dimensions so that optimal parameters must be selected for the fabrication of structurally sound component by WAAM process.

#### REFERENCES

- [1] X. Wang, S. Xu, S. Zhou, W. Xu, M. Leary, P. Choong, M. Qian, M. Brandt, Y. M. Xie, Topological design and additive manufacturing of porous metals for bone scaffolds and orthopaedic implants: A review. *Biomaterials* **83**, 127-141 (2016).
- [2] Z. Liu, B. He, T. Lyu, Y. Zou, A Review on Additive Manufacturing of Titanium Alloys for Aerospace Applications: Directed Energy Deposition and Beyond Ti-6Al-4V. *Jom.-J. Min. Met. Mat. S.* **73** (6), 1804-1818 (2021).
- [3] A. Zhakeyev, P. Wang, L. Zhang, W. Shu, H. Wang, J. Xuan, Additive Manufacturing: Unlocking the Evolution of Energy Materials. *Adv. Sci.* **4** (10) (2017).
- [4] R. Leal, F.M. Barreiros, L. Alves, F. Romeiro, J.C. Vasco, M. Santos, C. Marto, Additive manufacturing tooling for the automotive industry. *Int. J. Adv. Manuf. Tech.* **92** (5-8), 1671-1676 (2017).
- [5] P. Akbari, F. Ogoke, N.Y. Kao, K. Meidani, C.Y. Yeh, W. Lee, A.B. Farimani, MeltpoolNet: Melt pool characteristic prediction in Metal Additive Manufacturing using machine learning. *Addit. Manuf.* **55**, 102817 (2022).
- [6] D. Ding, F. He, L. Yuan, Z. Pan, L. Wang, M. Ros, The first step towards intelligent wire arc additive manufacturing: An automatic

- bead modelling system using machine learning through industrial information integration. *J. Ind. Inf. Integr.* **23**, 100218 (2021).
- [7] B. Wu, Z. Pan, D. Ding, D. Cuiuri, H. Li, J. Xu, J. Norrish, *Journal of Manufacturing Processes. J. Manuf. Process.* **35**, 127-139 (2018).
- [8] W.J. Sames, F.A. List, S. Pannala, R.R. Dehoff, S.S. Babu, The metallurgy and processing science of metal additive manufacturing. *Int. Mater. Rev.* **61** (5), 315-360 (2016).
- [9] Y. Zhang, L. Wu, X. Guo, S. Kane, Y. Deng, Y.G. Jung, J.H. Lee, J. Zhang, *Additive Manufacturing of Metallic Materials: A Review. J. Mater. Eng. Perform.* **27** (1), 1-13 (2018).
- [10] M. Dinovitzer, X. Chen, J. Laliberte, X. Huang, H. Frei, Effect of wire and arc additive manufacturing (WAAM) process parameters on bead geometry and microstructure. *Addit. Manuf.* **26**, 138-146 (2019).
- [11] A.S. Yildiz, K. Davut, B. Koc, O. Yilmaz, Wire arc additive manufacturing of high-strength low alloy steels: study of process parameters and their influence on the bead geometry and mechanical characteristics. *Int. J. Adv. Manuf. Technol.* **108** (11-12) 3391-3404 (2020).
- [12] A. Sharma, N. Arora, B.K. Mishra, Mathematical model of bead profile in high deposition welds. *J. Mater. Process. Technol.* **220**, 65-75 (2015).
- [13] A. Al-faruk, A. Hasib, N. Ahmed, U.K. Das, Prediction of Weld Bead Geometry and Penetration in Electric Arc Welding using Artificial Neural Networks. *Int. J. Mech. Mechatron. Eng.* **04**, 23-28 (2010).
- [14] J. Wanwan, Z. Chaoqun, J. Shuoya, T. Yingtao, W. Daniel, L. Wen, *Wire Arc Additive Manufacturing of Stainless Steels: A Review. Appl. Sci.* **10**, 1563 (2020).
- [15] W. Hackenhaar, J.A.E. Mazzaferro, F. Montevecchi, G. Campatelli, An experimental-numerical study of active cooling in wire arc additive manufacturing. *J. Manuf. Process.* **52**, 58-65 (2020).
- [16] U. Reisgen, R. Sharma, S. Mann, L. Oster, Increasing the manufacturing efficiency of WAAM by advanced cooling strategies. *Weld. World.* **64** (8), 1409-1416 (2020).
- [17] P.W. Fuerschbach, G.A. Knorovsky, A Study Of Melting Efficiency In Plasma-Arc And Gas Tungsten Arc-Welding. *Weld. J.* **70** (11), 287-297 (1991).
- [18] M.T. Andani, R. Dehghani, M.R.K. Ravari, R. Mirzaeifar, J. Ni, A study on the effect of energy input on spatter particles creation during selective laser melting process. *Addit. Manuf.* **20**, 33-43 (2018).
- [19] B. Fotovvati, S.F. Wayne, G. Lewis, E. Asadi, A Review on Melt-Pool Characteristics in Laser Welding of Metals. *Adv. Mater. Sci. Eng.* (2018).
- [20] B. Mezrag, F. Deschaux Beaume, S. Rouquette, M. Benachour, Indirect approaches for estimating the efficiency of the cold metal transfer welding process. *Sci. Technol. Weld. Join.* **23** (6), 508-519 (2018).
- [21] C. Cambon, S. Rouquette, I. Bendaoud, C. Bordreuil, R. Wimpory, F. Soulie, Thermo-mechanical simulation of overlaid layers made with wire + arc additive manufacturing and GMAW-cold metal transfer. *Weld. World.* **64** (8), 1427-1435 (2020).
- [22] C. Wang, X.P. Tan, S.B. Tor, C.S. Lim, Machine learning in additive manufacturing: State-of-the-art and perspectives. *Addit. Manuf.* **36**, 101538 (2020).
- [23] N.S. Johnson, P.S. Vulimiri, A.C. To, X. Zhang, C.A. Brice, B.B. Kappes, A. P. Stebner, Invited review: Machine learning for materials developments in metals additive manufacturing. *Addit. Manuf.* **36**, (2020).
- [24] H. Sondagar, S.S. Bhadauria, V.S. Sharma, Artificial neural network (ANN) based prediction of process parameters in additive manufacturing. *IOP Conf. Ser. Mater. Sci. Eng.* **1136** (1), 012026 (2021).
- [25] R. Pradhan, A.P. Joshi, M.R. Sunny, A. Sarkar, Performance of predictive models to determine weld bead shape parameters for shielded gas metal arc welded T-joints. *Mar. Struct.* **86**, 103290 (2022).
- [26] G.O. Barrionuevo, P.M. Sequeira-Almeida, S. Ríos, J.A. Ramos-Grez, S.W. Williams, A machine learning approach for the prediction of melting efficiency in wire arc additive manufacturing. *Int. J. Adv. Manuf. Technol.* **120** (5-6), 3123-3133 (2022).
- [27] R.F. Marmolejo, T.T. Siva, The shifting boxplot. A boxplot based on essential summary statistics around the mean. *Int. J. Psychol. Res.* **3** (1), 37-45 (2010).
- [28] A.C. Cameron, F.A.G. Windmeijer, An R-squared measure of goodness of fit for some common nonlinear regression models. *J. Econom.* **77** (2), 329-342 (1997).
- [29] D. Ding, C. Shen, Z. Pan, D. Cuiuri, H. Li, N. Larkin, S. Duin, Towards an automated robotic arc-welding-based additive manufacturing system from CAD to finished part. *CAD Comput. Aided Des.* **73**, 66-75 (2016).